J. Phys. B: At. Mol. Opt. Phys. 28 (1995) 2729–2744. Printed in the UK

Phase-dependent on- and off-shell effects in reflection of electrons from an impenetrable potential wall in a bichromatic laser field

S Varró† and F Ehlotzky‡

† Research Institute for Solid State Physics of the Hungarian Academy of Sciences, PO Box 49, H-1525 Budapest, Hungary

‡ Institute for Theoretical Physics, University of Innsbruck, A-6020 Innsbruck, Austria

Received 27 January 1995

Abstract. We consider the reflection of electrons by an infinitely high potential wall in the presence of a bichromatic laser field having two components of frequency ω and 2ω. Both components are out of phase by an angle φ. We evaluate the induced and inverse bremsstrahlung for this elementary scattering process and we discuss the coherent phase-control of the non-linear currents $j(n;\varphi)$ of electron reflection. If E_0 is the initial electron energy and $\hbar\omega$ the photon energy, two specific cases will be of interest: (a) $E_0 \gg \hbar\omega$ and (b) $E_0 \gtrsim \hbar\omega$, where in the latter case off-shell effects are particularly relevant. We shall relate our findings to the corresponding scattering of electrons by a hard sphere in a bichromatic field.

1. Introduction

Electron–atom scattering in a laser field is one of the processes which allows the investigation of multiphoton effects at comparatively low field intensities. The laser field introduces additional parameters, like its frequency ω, polarization ϵ, intensity I and its stochastic properties, which modify the basic scattering process and permit a deeper insight into it. A large number of papers have been written on this subject and surveys on the theoretical side of this problem can be found in the books by Mittleman [1] and Faisal [2] as well as in the review by Francken and Joachain [3]. The experimental situation is summarized in a recent review by Mason [4].

Recently, a new parameter, which can considerably modify multiphoton processes, has come into play. Since by modern laser technology one is able to produce higher harmonics of a laser field of sufficiently high power and to control the phase φ between the fundamental field and its harmonics, it has been suggested to consider multiphoton processes in a bichromatic field as a function of the relative phase φ of the two field components. Thus phase-dependent effects in multiphoton ionization and harmonic generation [5–1] and the phase control of molecular reactions [12–14] have been investigated. Moreover, the phase-dependent modulation of the lineshape of autoionizing resonances [15] and the phase control of resonance scattering in a bichromatic field [16] have been considered very recently.

Several years ago, we investigated the scattering of electrons by a hard sphere in a laser field [17], since it seemed to be the simplest boundary value problem, which can be solved exactly and analytically in the absence of the radiation field. However, the field destroys the original symmetry of the problem and we were not successful in solving the matching equations $\psi(R, t) = 0$ analytically, where R is the radius of the sphere and ψ the total

0953-4075/95/132729+16$19.50

wavefunction of the problem. Before attacking this problem again numerically, we want to consider here the much simpler process of electron reflection from a hard impenetrable wall in a laser field and we shall show that we can draw valuable conclusions which will also be pertinent to the three-dimensional case. In addition, we shall consider this problem in a bichromatic field of frequencies ω and 2ω and we shall investigate the coherent phase-control of the non-linear probability currents $j(n;\varphi)$ of reflected electrons, corresponding to induced and inverse bremsstrahlung. We shall relate our findings to the results of our recent investigations on potential scattering of electrons in a bichromatic field in the first Born approximation [18, 19]. If E_0 is the initial electron energy and $\hbar\omega$ the photon energy, we shall discuss, in particular, the following two cases: (a) $E_0 \gg \hbar\omega$, which is the so called low-frequency limit, and (b) $E_0 \gtrsim \hbar\omega$, in which case off-shell effects become of great importance. As far as we know, this will be the first explicit investigation of the phase control of off-shell effects. As we shall see, these effects are particularly large near the minima of the electron reflection probability currents $j(n;\varphi)$ and they vary, moreover, very strongly with the phase φ.

2. Model

Since the electron energies which we shall be considering are in the range from 100 to a few eV and the laser intensities chosen will be far below the critical values, we may treat the problem non-relativistically. Moreover, the emission and absorption processes only take place in the vicinity of the reflecting wall and therefore the use of the dipole approximation will be sufficient. We assume the reflecting wall to be located in the (x, y) plane of our coordinate system and we take the electrons to impinge onto the wall from the left in the positive z direction, while their motion is restricted to the domain $z < 0$. The bichromatic radiation field will be linearly polarized in the z direction so that the polarization vector $\epsilon = e_z$ and for the ingoing electron of energy E_0 the momentum will be $p_0 = p_0 e_z$. In this configuration there is no motion of the electron in the (x, y) directions and our problem is a purely one-dimensional one. For the description of the bichromatic laser field we choose the classical field representation in which the vector potential is given by

$$A(t) = (cF/\omega)e_z \cos\omega t + \left(cF_2/2\omega\right)e_z \cos(2\omega t + \varphi). \tag{1}$$

In this field the well known Gordon–Volkov solutions read [20, 21]

$$\psi_p = \exp\{-(\mathrm{i}/\hbar)[Et - p(z - \alpha \sin\omega t - \alpha_2 \sin(2\omega t + \varphi))]\} \tag{2}$$

where α and α_2 are the amplitudes of the classical electron oscillations in the two radiation fields, given by

$$\begin{aligned} &\alpha = \mu c/\omega \qquad \mu = eF/mc\omega \\ &\alpha_2 = \mu_2 c/2\omega \qquad \mu_2 = eF_2/mc2\omega \end{aligned} \tag{3}$$

with μ and μ_2 being the intensity parameters of the two fields. The on-shell relation in the two laser fields reads

$$p = [2m(E - \sigma)]^{1/2} \qquad \sigma = \sigma_1 + \sigma_2 \tag{4}$$

where σ is the total laser induced AC Stark shift with

$$\sigma_1 = \tfrac{1}{4}mc^2\mu^2 \qquad \sigma_2 = \tfrac{1}{4}mc^2/\mu_2^2. \tag{5}$$

In the Gordon–Volkov solution (2) we have neglected the A^2 part of the laser interaction except for the Stark shift σ. The neglected part generally does not contribute to scattering processes. Since, later on, we would like to put an emphasis on the phase-dependent effects, we shall choose $F_2 = F$, so that in (3) we get $\mu_2 = \frac{1}{2}\mu$ and in (4) we find $\sigma = \frac{5}{4}\sigma_1$. Moreover, the numerical value of μ can be evaluated from the formula $\mu = 10^{-9}[I/\mathrm{W\ cm^{-2}}]^{1/2}[\hbar\omega/\mathrm{eV}]^{-1}$ where I is the laser intensity in W cm^{-2} and $\hbar\omega$ is the photon energy in eV.

The wavefunction (2) is an exact solution of the Schrödinger equation for an electron moving in the field (1), but it clearly does not fulfil the general boundary condition at the reflecting wall

$$\psi(z = 0,\ t) = 0. \tag{6}$$

Even the superposition of an ingoing and a reflected Gordon–Volkov wave will not be sufficient. As we have shown in one of our earlier investigations [22], it will be necessary to make the following Floquet-type of ansatz in order to consistently solve the matching problem

$$\psi(z,\ t) = \psi_{p_0}^{(+)} - \sum_{n=-\infty}^{+\infty} R_n \psi_{p_n}^{(-)} \tag{7}$$

where

$$\psi_{p_0}^{(+)} = \exp\bigl[-(\mathrm{i}/\hbar)\bigl(E_0 t - p_0 z\bigr)\bigr]\exp\bigl[-\mathrm{i}a_0 \sin\omega t - \mathrm{i}b_0 \sin(2\omega t + \varphi)\bigr] \tag{8}$$

$$\psi_{p_n}^{(-)} = \exp\bigl[-(\mathrm{i}/\hbar)\bigl(E_0 + n\hbar\omega\bigr)t + p_n z\bigr]\exp\bigl[\mathrm{i}a_n \sin\omega t + \mathrm{i}b_n \sin(2\omega t + \psi)\bigr] \tag{9}$$

with

$$p_n = \bigl[2m\bigl(E_0 + n\hbar\omega - \sigma\bigr)\bigr]^{1/2} \tag{10}$$

$$a_n = p_n\alpha/\hbar \qquad b_n = p_n\alpha_2/\hbar. \tag{11}$$

In the ansatz (7), $\psi_{p_0}^{(+)}$ represents an incoming electron propagating in the positive z direction with initial energy E_0 and momentum p_0 while $\psi_{p_n}^{(-)}$ represents the components of the reflected electron wave propagating to the left with the energies $E_0 + n\hbar\omega$ and momenta $-p_n$. An n-photon process is associated with each of the latter components. Of course, if $E_0 + n\hbar\omega - \sigma < 0$, then p_n is purely imaginary and the corresponding wave component decays exponentially from the origin for $z < 0$ (known as an evanescent wave). These components represent closed channels of the scattering process.

Summarizing, the ingoing electron is inelastically scattered at the wall at $z = 0$, due to the presence of the field (1), and absorbs ($n > 0$) or emits ($n < 0$) n photons $\hbar\omega$. It is worth mentioning that in our semiclassical description of the radiation interaction with two fields of commensurable frequencies ω and 2ω it cannot be decided from which field component a particular energy increase (or decrease) originates.

Since (8) and (9) are exact solutions of the Schrödinger equation, (7) also is an exact solution and the unknown reflection coefficients R_n can now be obtained from the boundary condition (6) which yields for $z = 0$ and all t

$$\psi_{p_0}^{(+)}(0,\ t) = \sum_n R_n \psi_{p_n}^{(-)}(0,\ t). \tag{12}$$

On account of (8) and (9) we can expand both sides of (12) into a Fourier series in t and equate the corresponding Fourier coefficients of both sides. This yields the following infinite set of linear algebraic equations for the reflection coefficients R_k

$$B_n(a_0,\ b_0,\ \varphi) = \sum_{k=-\infty}^{+\infty} B_{n-k}(-a_k,\ -b_k;\ \varphi) R_k. \tag{13}$$

Here we have introduced the generalized Bessel functions defined by

$$B_n(x,\ y;\ \varphi) = \sum_{\lambda=-\infty}^{+\infty} J_{n-2\lambda}(x) J_\lambda(y) \exp(\mathrm{i}\lambda\varphi) \tag{14}$$

which can be obtained as Fourier coefficients of the following generating function

$$\exp[\mathrm{i}x \sin\alpha + \mathrm{i}y \sin(2\alpha + \varphi)] = \sum_{n=-\infty}^{+\infty} B_n(x,\ y;\ \varphi) \exp(\mathrm{i}n\alpha) \tag{15}$$

and which can be used to easily derive the following addition theorem

$$\sum_{\lambda=-\infty}^{+\infty} B_{n-\lambda}(x_1,\ y_1;\ \varphi) B_\lambda(x_2,\ y_2;\ \varphi) = B_n(x_1 + x_2,\ y_1 + y_2;\ \varphi). \tag{16}$$

By means of this addition theorem, the matching equation (13) can be put into a more tractable form

$$B_n(a_n + a_0,\ b_n + b_0;\ \varphi) = \sum_{k=-\infty}^{+\infty} B_{n-k}(a_n - a_k,\ b_n - b_k;\ \varphi) R_k. \tag{17}$$

Here the matrix $M(\varphi) = \{M_{n,k}(\varphi)\} \equiv \{B_{n-k}(a_n - a_k,\ b_n - b_k;\ \varphi)\}$ has some symmetry properties which the matrix on the right-hand side of (13) does not have. First of all, its diagonal elements are all equal to unity, $M_{n,n}(\varphi) = 1$. Next, the transposed matrix, $M^{\mathrm{T}}(\varphi)$, is related to the original matrix $M(\varphi)$ by the relation $M^{\mathrm{T}}(\varphi) = M(-\varphi)$ and hence $M(\varphi = 0)$ is a symmetric matrix. Finally, if $E_0 \gg \hbar\omega$, then in a wide interval of indices n and k, a_n, a_k, b_n, b_k are all real on account of (10) and (11). Consequently, the properly truncated matrix $\tilde{M}(\varphi)$ is self-adjoint, i.e. $\tilde{M}^{\mathrm{T}^*}(\varphi) = \tilde{M}^*(-\varphi) = \tilde{M}(\varphi)$.

Besides the advantageous mathematical properties of the kernel matrix M listed, the relation (17) has a very transparent physical interpretation. In fact, $B_n(a_n + a_0,\ b_n + b_0;\ \varphi)$ represents the first-order Born amplitude of the n-photon stimulated bremsstrahlung during the one-dimensional backscattering from the initial state and it is an on-shell amplitude. Similarly, $B_{n-k}(a_n - a_k,\ b_n - b_k;\ \varphi)$ are the off-shell Born amplitudes of the intermediate processes in which an electron of momentum p_k scatters to the state with momentum p_n, while simultaneously $n - k$ photons are absorbed (or emitted). According to (17), the

convolution of the true reflection coefficients with the Born amplitudes of the intermediate scattering yields the first-order Born amplitude of a scattering from the initial state. In the limit of low laser frequencies, $\hbar\omega \ll E_0$, we find by means of (3), (10) and (11) the approximation

$$B_{n-k}(a_n - a_k,\ b_n - b_k; \varphi) \simeq B_{n-k}\big[(n-k)\mu/\beta_0, (n-k)\mu_2/\beta_0; \varphi\big] \tag{18}$$

where $\beta_0 = v_0/c$, with v_0 being the initial velocity of the electron. If, moreover, the laser intensity is so low that $\mu/\beta_0 \ll 1$ and $\mu_2/\beta_0 \ll 1$, we obtain from (18) the approximation $B_{n-k}(a_n - a_k,\ b_n - b_k; \varphi) \simeq \delta_{n,k}$ and hence we find from (17) the approximate solution

$$R_n \simeq B_n(a_n + a_0,\ b_n + b_0; \varphi) \tag{19}$$

which in the general case, however, is much too crude an approximation, since in this approximation off-shell effects are neglected.

Unfortunately, in the general case of laser frequencies and intensities, (17) does not permit an analytic solution and hence we solve this problem numerically for various values of the input parameters. As soon as we know the reflection coefficients R_n, then the components of the probability current associated with the different n-photon backscattering processes are given by $p_n|R_n|^2$ (apart from some normalization factor). Of course, the evanescent components, for which $p_n = \mathrm{i}|p_n|$ and which decay exponentially from the origin, correspond to closed channels. Hence, the incoming current j_0 is distributed into the reflected partial currents j_n corresponding to open channels. Since, according to (10), $p_n = [2m(E_0 + n\hbar\omega - \sigma)]^{1/2}$, there must exist a smallest value for the index, n, $n_0 \gtrless 0$ say, for which p_n is still real, whereas for $n_0 - 1$, p_n becomes purely imaginary. Of course, the value of n_0 will also depend on the size of the AC Stark shift σ. Therefore, the distribution of the reflected currents will satisfy the sum rule

$$\sum_{n=n_0}^{\infty} p_n |R_n|^2 / p_0 = 1. \tag{20}$$

In our numerical analysis, it will be of interest to compare the reflected currents in a bichromatic field with those for a monochromatic plane wave. The latter problem was investigated many years ago by Berson and Bondars [23]. In this case we obtain for the reflection coefficients R_n instead of (17) the relation

$$J_n(a_n + a_0) = \sum_{k=-\infty}^{+\infty} J_{n-k}(a_n - a_k) R_k \tag{21}$$

which also can only be solved numerically.

3. Numerical example

In the figures presented below, the renormalized currents $p_n|R_n|^2/p_0$ will be denoted by $j(n)$, if a monochromatic field is present, and the partial currents in a bichromatic field will be called $j(n; \varphi)$. First we shall consider the case (a) in which $E_0 \gg \hbar\omega$, corresponding to the low-frequency limit, and then the case (b), where $E_0 \gtrsim \hbar\omega$ and where the off-shell effects are important.

(a) Here we only need to consider the on-shell Born approximation (19), in the arguments of which we may even drop the index n. Thus we get for a single field from (21) $j(n) = J_n^2(2a_0)$ and for a bichromatic field from (19) $j(n;\varphi) = |B_n(2a_0, 2b_0;\varphi)|^2$ as the probability currents of electron reflection. Choosing $E_0 = 100$ eV, $\hbar\omega = 1$ eV and a laser intensity $I = 10^{11}$ W cm^{-2} (or equivalently $E_0 = 10$ eV, $\hbar\omega = 0.1$ eV and $I = 10^8$ W cm^{-2}), where the harmonic field is assumed to have the same intensity as the fundamental (i.e. $F_2 = F$ in (3)), we obtain by means of (3), (11) and (14) the data depicted in figure 1. In (a) we show $j(n)$ for a single frequency ω and in (b) $j(n, 0)$, (c) $j(n;\pi/2)$ and (d) $j(n, \pi)$. If we compare these results with what we found in our earlier work on three-dimensional potential scattering of electrons in a bichromatic field [18, 19], we find essentially the same phase dependence of the electron spectra, since these results only depend on the specific values of the arguments of the ordinary, or generalized, Bessel functions and not on the specific scattering geometry or boundary conditions. Thus, in the low-frequency limit our one-dimensional problem yields the same results as the three-dimensional counterpart.

(b) In this case we choose as initial electron energy $E_0 = 3.1$ eV and as photon energy $\hbar\omega = 1$ eV. As the on-shell approximation we may again consider the Born term (19), retaining now the n-dependence of the arguments of the generalized Bessel functions (or, for a single field, the argument of the ordinary Bessel functions). Thus we find for a single field as the on-shell approximation for the reflected probability currents $j^{(0)}(n) = (p_n/p_0)J_n^2(a_n + a_0)$ and for the bichromatic field $j^{(0)}(n, \varphi) = (p_n/p_0)|B_n(a_n + a_0, b_n + b_0;\varphi|^2$. Here we get, even for a single field, an asymmetry of the reflected electron spectra, depending on $n < 0$ or $n > 0$. Moreover, we shall have channel closing (and the appearance of evanescent waves) for $E + n\hbar\omega - \sigma < 0$, so that, with increasing laser field intensity and thus increasing Stark shift σ, channel closing will take place at less negative values of n. Hence, the spectra will be different from what we have obtained in the low frequency limit (a), shown in our examples of figure 1, but there will remain some resemblance in the oscillatory behaviour of $j^{(0)}(n)$ and $j^{(0)}(n;\varphi)$ as a function of n and φ. For a single field, this oscillatory behaviour can be well understood on account of the properties of the ordinary Bessel functions, which show, for a fixed value of the argument, rather large oscillations for small n, but with increasing n, these oscillations gradually level off, which can be very nicely seen in the diagram of figure 80 in the tables of Jahnke *et al* [24]. In the case of a bichromatic field, the situation appears to be similar, as we shall see below. As long as we only consider the above mentioned on-shell approximation, the results for the probability currents of reflection $j^{(0)}(n)$ and $j^{(0)}(n;\varphi)$ will be independent of the specific scattering geometry and boundary conditions, since the results only depend on the specific values of the arguments of the Bessel functions. This situation changes definitely if we include the off-shell effects into our considerations. These depend on the specific boundary conditions and on the scattering geometry. The inclusion of these effects requires the numerical inversion of (17) or (21) to exactly evaluate the reflection coefficients R_n. As it turns out, however, the off-shell effects are in general particularly large for those values of n where the exact reflected currents, denoted by $j(n)$ for a single field and $j(n;\varphi)$ for a bichromatic field, are rather small. Hence, we may expect that even with regard to the off-shell effects we may get some insight from our simple, one-dimensional model calculation in relation to the three-dimensional scattering of electrons by a hard sphere in a bichromatic field, in particular, if backward scattering is considered and the hard sphere is approximated by an impenetrable tangential plane. As a measure of the off-shell effects, we introduce the quantity $\mathrm{off}(n) = [j(n) - j^{(0)}(n)]/j^{(0)}(n)$ for a single field and $\mathrm{off}(n;\varphi) = [j(n;\varphi) - j^{(0)}(n;\varphi)]/j^{(0)}(n;\varphi)$ for a bichromatic field. In the following figures, we first show $j(n)$ and $j(n;\varphi)$ for two different laser field intensities

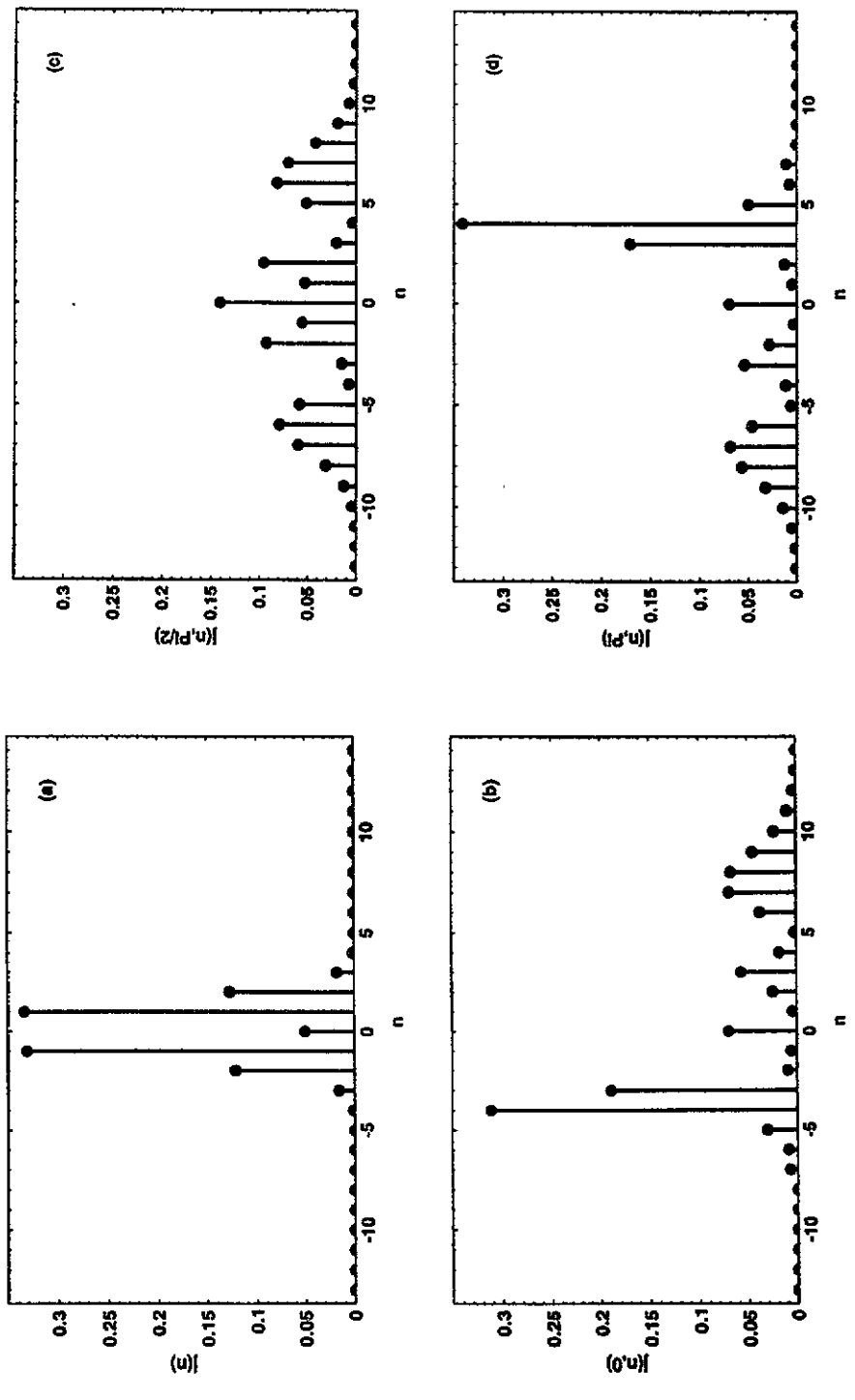

Figure 1. The spectra of reflected electrons in the low-frequency limit for $E_0 = 100$ eV, $\hbar\omega = 1$ eV and $I = 10^{11}$ W cm^{-2}. (a) refers to $j(n)$ for a single field, (b) to $j(n;0)$, (c) to $j(n,\frac{1}{2}\pi)$ and (d) to $j(n;\pi)$. These spectra are very similar to what has been found in [18, 19].

and various phases φ and we then depict off(n) and off(n; φ) for the same parameters. As said before, $E_0 = 3.1$ eV and $\hbar\omega = 1$ eV are chosen.

In figure 2(a) and (b) the laser intensity has been chosen as $I = 5 \times 10^{11}$ W cm^{-2}, where (a) shows the reflected non-linear currents $j(n)$ for a single frequency as a function of n, while (b) represents the currents $j(n, 0)$ for $\varphi = 0$ with both frequencies present. Similarly, figure 2(c) and (d) present data for $I = 5 \times 10^{12}$ W cm^{-2} with (c) corresponding to $j(n)$ for one frequency and (d) showing $j(n, 0)$ for two frequencies. Comparing (a) with (b) and (c) with (d), respectively, we first of all recognize an enormous change of the spectra in going from a monochromatic to a bichromatic field and, moreover, with increasing intensity, the smallest number n_0 of open channels begins to increase due to the increase of the AC Stark shift σ in (10). While in figure 1(b), $n_0 = -3$, in figure 1(d) we get $n_0 = -2$. We also recognize that in a bichromatic field the spectrum expands into higher values of the non-linear order n.

In figures 3, 4 and 5 the intensity has been chosen $I = 5 \times 10^{12}$ W cm^{-2} and in these figures the currents $j(n; \varphi)$ for two fields are depicted for various values of the phase φ. Thus, in figures 3(a)–(d) φ has been chosen as 0, $\frac{1}{4}\pi$, $\frac{1}{2}\pi$ and $\frac{3}{4}\pi$ respectively, in figures 4(a)–(d) we have $\varphi = \pi$, $\frac{5}{4}\pi$, $\frac{3}{2}\pi$ and $\frac{7}{4}\pi$ respectively and finally in figures 5(a)–(d) we took $\varphi = \frac{1}{3}\pi$, $\frac{2}{3}\pi$, $\frac{4}{3}\pi$ and $\frac{5}{3}\pi$. In all these figures we find as common features of the current distributions that for large values of the non-linear order n the currents $j(n; \varphi)$ are rather continuously distributed with a maximum somewhere between $n = 10$ and $n = 15$, whereas for small n, the values of $j(n; \varphi)$ very strongly depend on φ and there are rather dramatic changes of $j(n; \varphi)$ as a function of n. A particularly dramatic current distribution can be found in figure 4(a) for $\varphi = \pi$, where $j(5, \pi)$, $j(6, \pi)$, $j(7, \pi)$ are dominant whereas all other reflected currents are strongly suppressed.

The above general features of $j(n)$ and $j(n; \varphi)$ can be well understood, if one considers the on-shell approximations $j^{(0)}(n)$ and $j^{(0)}(n; \varphi)$. The behaviour of $j^{(0)}(n)$ has been discussed before, so we concentrate on $j^{(0)}(n; \varphi)$. If $\varphi = 0$, the two Bessel functions $J_{n-2\lambda}$ and J_λ in (14) will yield large contributions and strong interferences if $n - 2\lambda$ and λ are small and close to each other, yielding large variations of $j(n; 0)$ for small n. If n increases, either $n - 2\lambda$ or λ will be large, and the interferences will level off and $j(n; 0)$ will decrease and oscillate less dramatically, as our figures demonstrate. If the φ-dependence is included, this means that φ acts as an additional control parameter of the interferences between $J_{n-2\lambda}$ and J_λ. Hence, the enormous phase effects shown in the above figures are also plausible.

In figures 6–8 we have plotted $j(n)$ and $j(n; \varphi)$ for the same intensity $I = 5 \times 10^{12}$ W cm^{-2} as above and for the same phase values. On top of this background we show the off-shell effects, defined by off(n) and off(n; φ) previously, in order to show the inter-relation between these quantities.

In figure 6 we show off(n), marked by crosses, on the background of $20 \times j(n)$, marked by dots, as a function of n. As remarked before, we see that off(n) is particularly large at the minima of $j(n)$. The largest values are off(-1) = 192.4 and off(2) = 7.4. As expected, the off-shell effects are particularly large close to channel closing at $n = -2$.

In figure 7 we show off(n; φ) and $20 \times j(n; \varphi)$ with the same markings as in figure 6. In (a) $\varphi = 0$ and off(4; 0) = 8.3 is the maximum value of the off-shell effect, similarly in (b) $\varphi = \frac{1}{4}\pi$ and off(4; $\frac{1}{4}\pi$) = 7.8; in (c) $\varphi = \frac{1}{2}\pi$ and off(-2, $\frac{\pi}{2}$) = 25.2; and in (d) $\varphi = \frac{3}{4}\pi$ and off(-2, $\frac{3}{4}\pi$) = 6.7. As we can see, the off-shell effects are strongly dependent on φ. Although their maxima are still close to the minima of the reflected currents, their maximum values need not be close to channel closing at $n = -2$, but they may occur at larger values of n, while, on the other hand, the off-shell effects may be suppressed near channel closing, as is the case for $\varphi = 0$, figure 7(a).

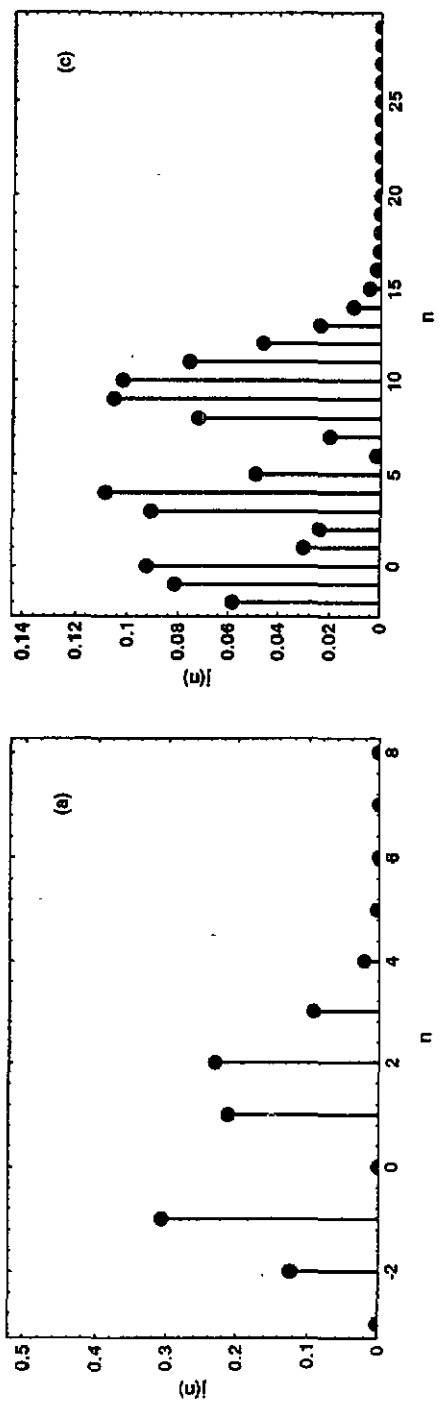

Figure 2. For initial electron energy $E_0 = 3.1$ eV and photon energy $\hbar\omega = 1$ eV in (a) and (b) for a laser intensity $I = 5 \times 10^{11}$ W cm^{-2} the reflected currents $j(n)$ and $j(n, 0)$ respectively are shown and similarly in (c) and (d) for a laser intensity $I = 5 \times 10^{12}$ W cm^{-2} the currents $j(n)$ and $j(n, 0)$. Observe the *different scales in (a) and (b) and (c) and (d).*

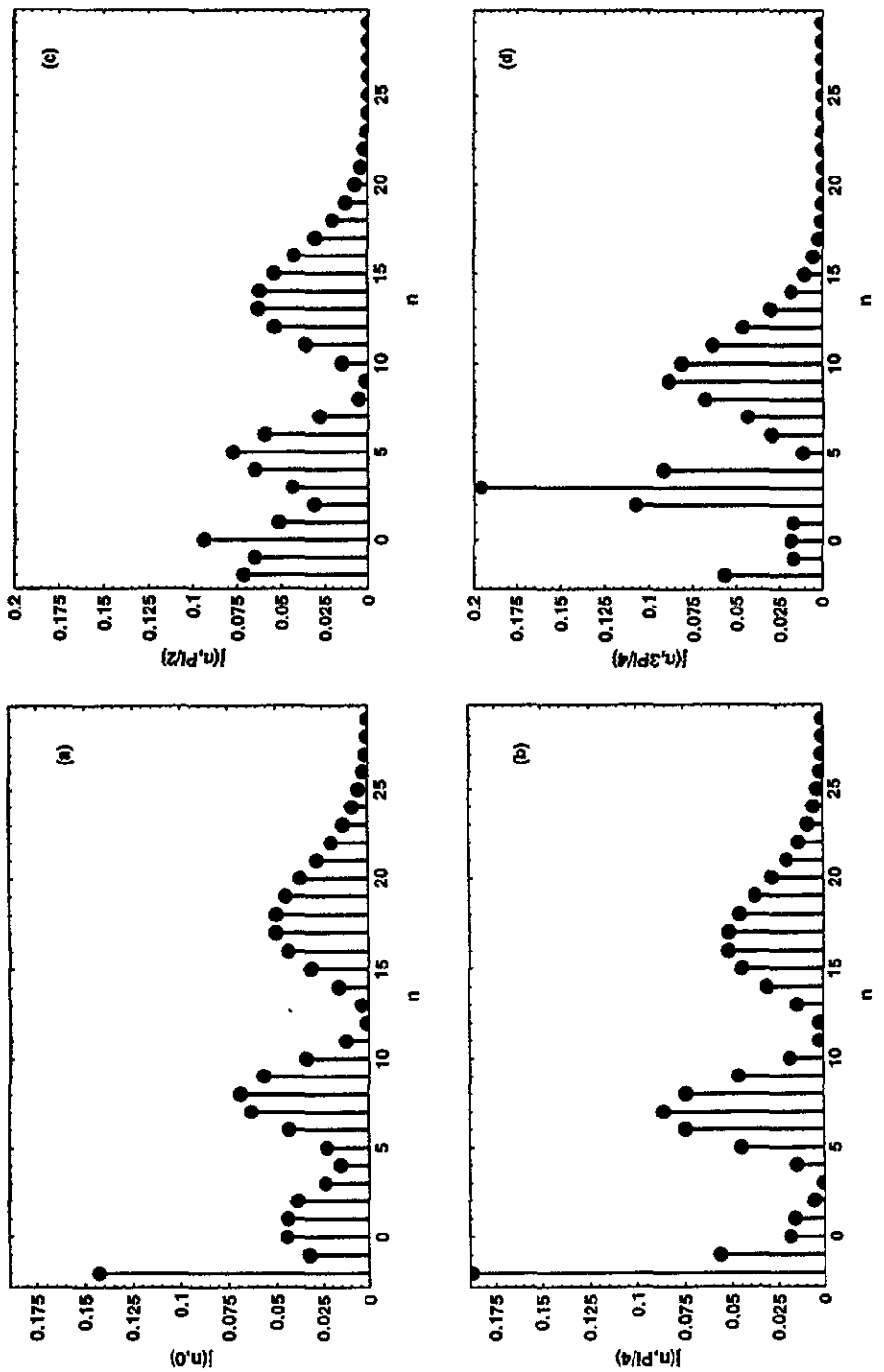

Figure 3. $E_0 = 3.1$ eV, $\hbar\omega = 1$ eV and $I = 5 \times 10^{12}$ W cm^{-2} and the reflected currents $j(n, \varphi)$ are shown in (a) for $\varphi = 0$, (b) $\varphi = \frac{1}{4}\pi$, (c) $\varphi = \frac{1}{2}\pi$ and (d) $\varphi = \frac{3}{4}\pi$.

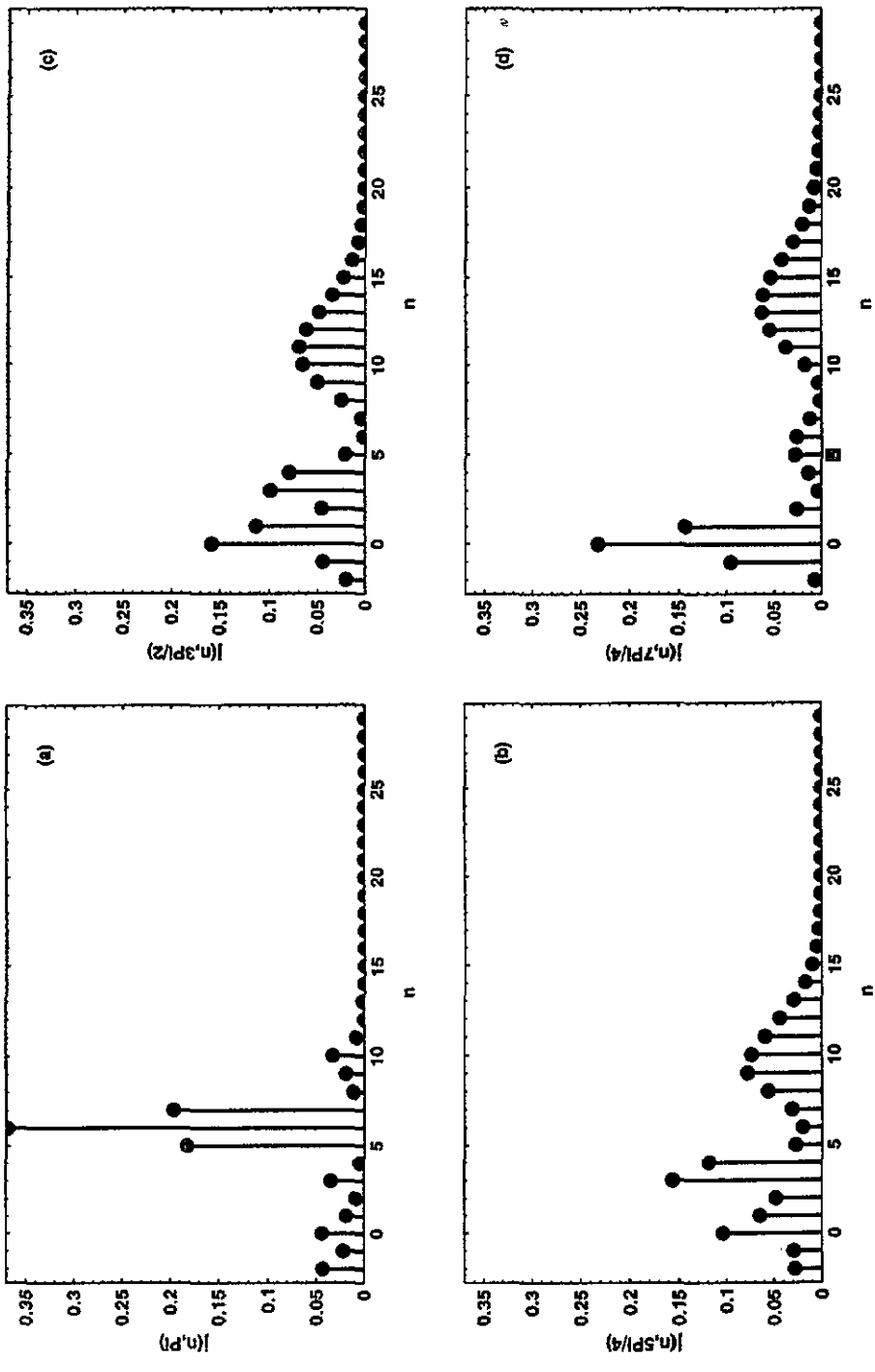

Figure 4. For the same values of E_0, $\hbar\omega$ and I as in figure 2, this figure presents $j(n, \varphi)$ in (a) for $\varphi = \pi$, (b) $\varphi = \frac{5}{4}\pi$, (c) $\varphi = \frac{3}{2}\pi$ and (d) $\varphi = \frac{7}{4}\pi$.

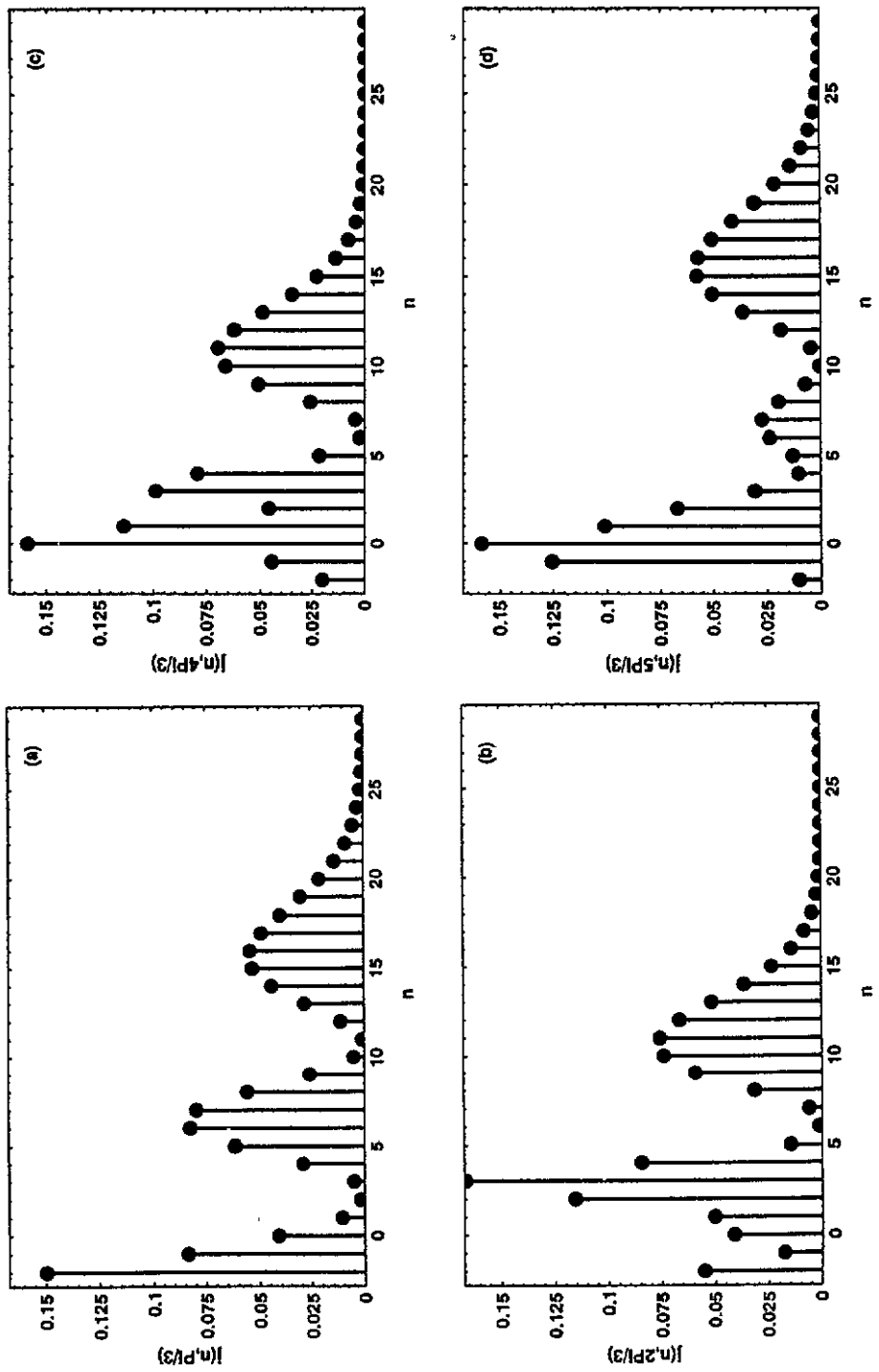

Figure 5. Here $j(n, \varphi)$ is presented in (a) for $\varphi = \frac{1}{3}\pi$, (b) $\varphi = \frac{2}{3}\pi$, (c) $\varphi = \frac{4}{3}\pi$ and (d) $\varphi = \frac{5}{3}\pi$.

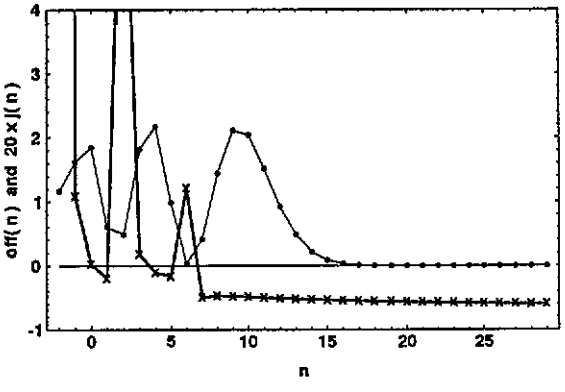

Figure 6. Here we depict $20 \times j(n)$ (dots) and off(n) (crosses) for a single field with intensity $I = 5 \times 10^{12}$ W cm^{-2}. The off-shell effects are particularly large at the minima of $j(n)$, having their largest value at $n = -1$, off$(-1) = 192.4$ near channel closing.

Similarly, we show in figure 8 off$(n; \varphi)$ and $20 \times j(n; \varphi)$. (a) refers to $\varphi = \frac{1}{2}\pi$, with a maximum value for off$(-1, \frac{1}{2}\pi) = 25.5$; (b) refers to $\varphi = \frac{5}{4}\pi$, with a maximum at off$(-1; \frac{5}{4}\pi) = 6.4$; (c) $\varphi = \frac{3}{2}\pi$, maximum at off$(9; \frac{3}{2}\pi) = 9$; and (d) $\varphi = \frac{7}{4}\pi$, maximum at off$(11; \frac{7}{4}\pi) = 67.8$. Hence, we see, in particular at the last value of φ, how the off-shell effects may extend to comparatively large values of n very far away from channel closing, which is very different from what we found in figure 6 for a single field. So the phase control of the off-shell effects can be quite appreciable.

4. Conclusions

In the present paper, we considered the reflection of electrons by an infinitely high potential wall, while a laser field is present. For comparison, we considered the probability currents of reflection $j(n)$ for a single field mode and, at the same time, $j(n; \varphi)$ for a bichromatic field. Two cases have been investigated in detail: (a) the low-frequency problem, in which the initial electron energy E_0 is much larger than the photon energy. Here the on-shell amplitudes yield the dominant contributions and the spectrum of the reflected currents is about the same as in a three-dimensional scattering problem in a laser field. In the case (b), in contrast, E_0 was of the same order of magnitude as $\hbar\omega$, and here the off-shell effects are of importance, which now depend very much on the specific boundary conditions and on the scattering geometry. Nevertheless, we were able to draw some general conclusions on the behaviour of the off-shell effects, which are particularly large, when the reflected currents are small, although there are exceptions. In particular, while in the case of a single field, off-shell effects are dominant close to channel closing, in a bichromatic field for particular phases φ the off-shell effects may be dominant for comparatively large values of the non-linear order n. On the whole, the coherent phase control of the off-shell effects is quite appreciable.

Acknowledgments

This work has been supported by the East–West Program of the Austrian Academy of

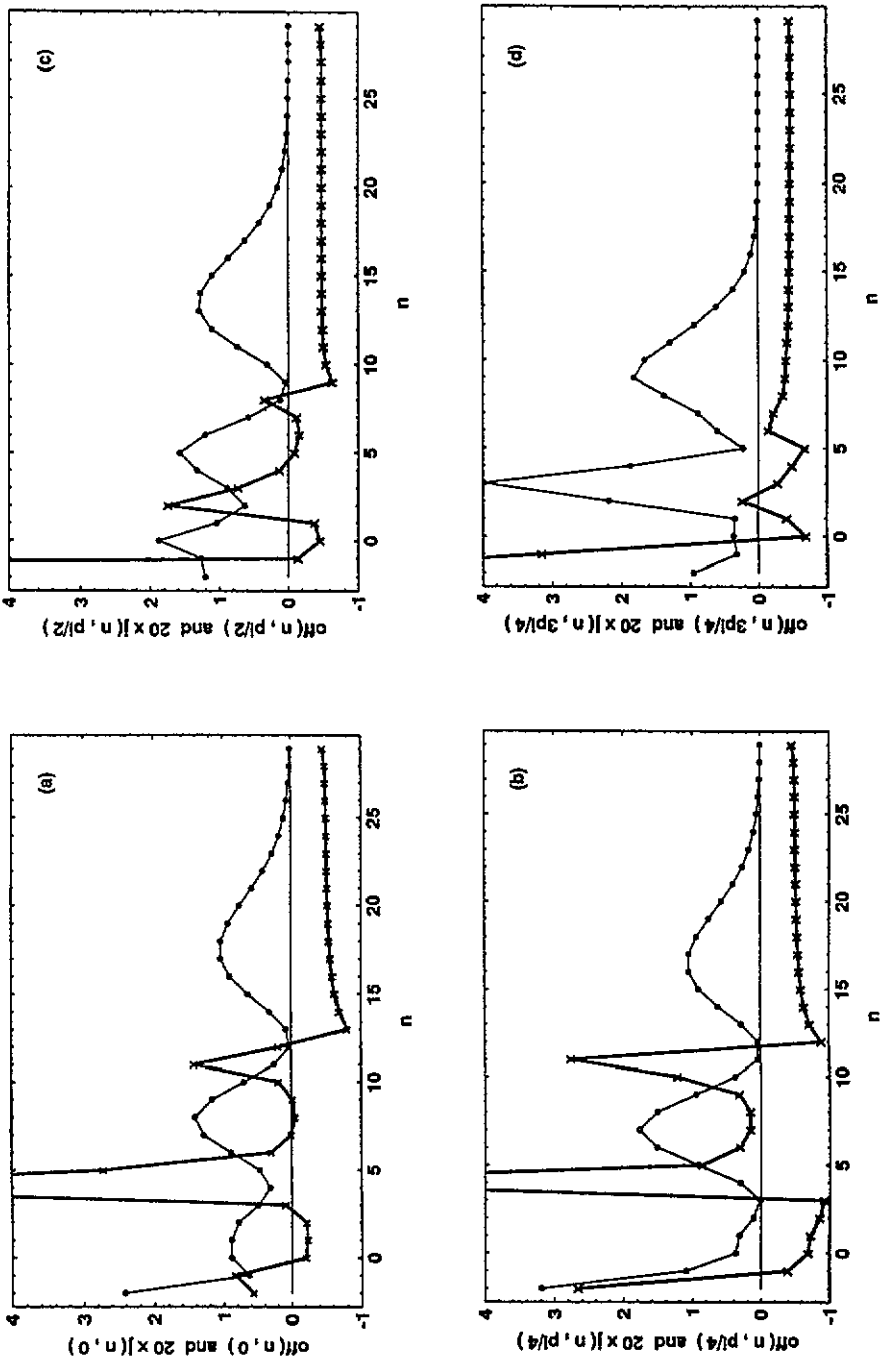

Figure 7. For the same intensity $20 \times f(n;\varphi)$ and $\mathrm{off}(n;\varphi)$ are shown for (a) $\varphi = 0$, (b) $\varphi = \frac{1}{4}\pi$, (c) $\varphi = \frac{1}{2}\pi$ and (d) $\varphi = \frac{3}{4}\pi$. A particularly large off-shell effect is for $\varphi = \frac{1}{2}\pi$ and $n = -2$, where $\mathrm{off}(-2, \frac{1}{2}\pi) = 25.2$ which is at channel closing, but there are maxima also found for larger $n = 4$ at $\varphi = 0$ and $\frac{1}{4}\pi$.

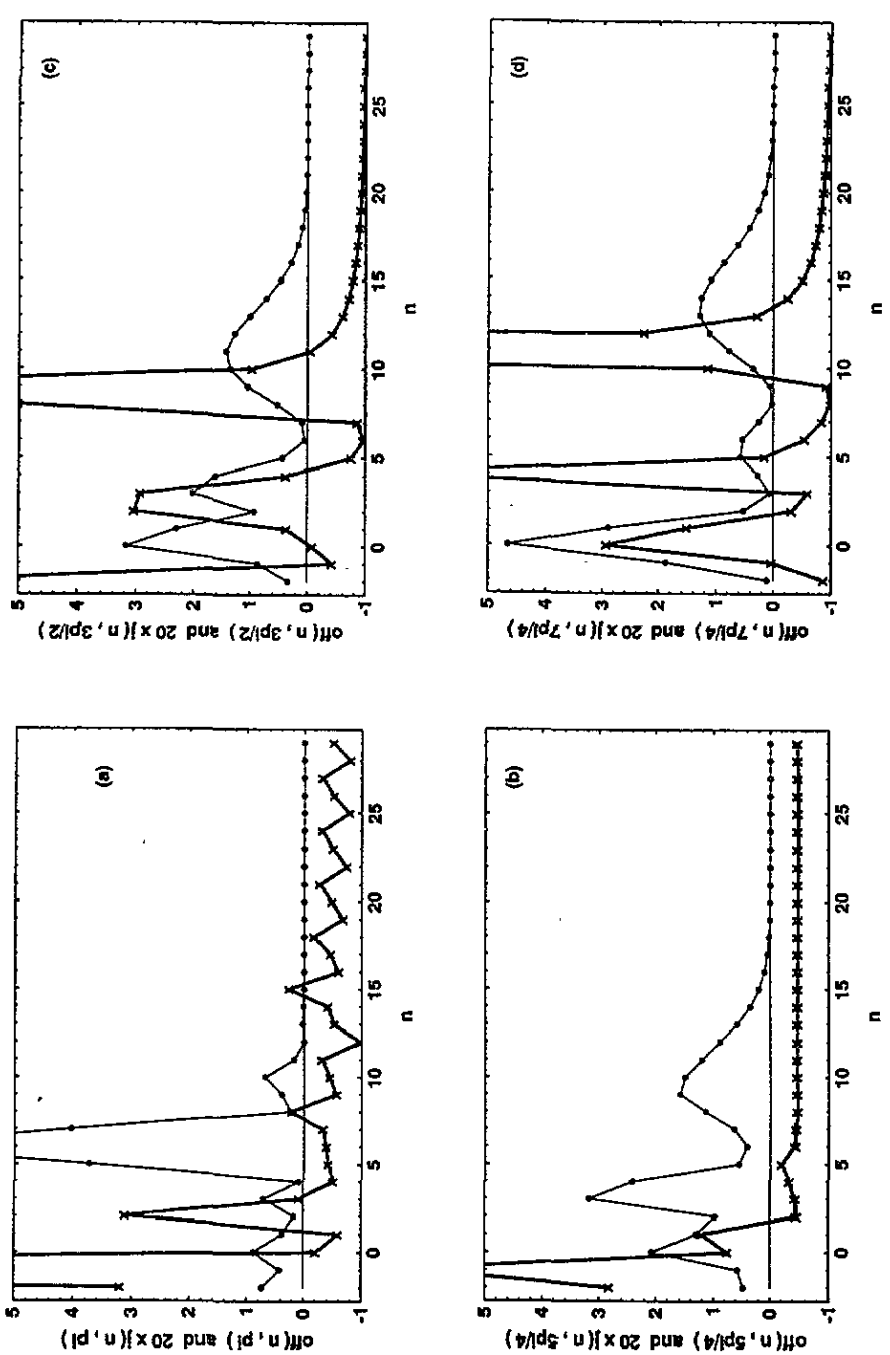

Figure 8. Here $20 \times j(n;\varphi)$ and $\mathrm{off}(n;\varphi)$ are depicted for (a) $\varphi = \frac{1}{2}\pi$, (b) $\varphi = \frac{5}{4}\pi$, (c) $\varphi = \frac{3}{2}\pi$ and (d) $\varphi = \frac{7}{4}\pi$. A particularly large off-shell effect is found rather far away from channel closing for $\varphi = \frac{7}{4}\pi$ at $n = 11$ with $\mathrm{off}(11, \frac{7}{4}\pi) = 67.8$.

Sciences and by the Austrian Ministry of Science and Research under contract no 45.732/2-IV/6/94. Moreover, one of us (SV) acknowledges the support of the Hungarian OTKA Foundation under project no 2936.

References

[1] Mittleman M H 1993 *Introduction to the Theory of Laser-Atom Interactions* 2nd edn (New York: Plenum)
[2] Faisal F H M 1987 *Theory of Multiphoton Processes* (New York: Plenum)
[3] Francken P and Joachain C J 1990 *J. Opt. Soc. Am.* B **7** 554
[4] Mason N J 1993 *Rep. Prog. Phys.* **56** 1275
[5] Müller H G, Bucksbaum P H, Schumacher D W and Zavriyev A 1990 *J. Phys. B: At. Mol. Opt. Phys.* **23** 2761
[6] Chen C and Elliot D S 1990 *Phys. Rev. Lett.* **65** 1737
Yien Y Y, Chen C and Elliot D S 1992 *Phys. Rev. Lett.* **69** 2353
[7] Szöke A, Kulander K C and Bardsley J N 1991 *J. Phys. B: At. Mol. Opt. Phys.* **24** 3165
[8] Potvliege R M and Smith P H G 1991 *J. Phys. B: At. Mol. Opt. Phys.* **24** L641; 1992 *J. Phys. B: At. Mol. Opt. Phys.* **25** 2501; 1994 *Phys. Rev.* A **49** 3110
[9] Schafer K J and Kulander K C 1992 *Phys. Rev.* A **45** 8026
[10] Perry M D and Crane J K 1993 *Phys. Rev.* A **48** R4051
[11] Protopapas M, Knight P L and Burnett K 1994 *Phys. Rev.* A **49** 1945
[12] Shapiro M, Hepburn J W and Brunner P 1988 *Chem. Phys. Lett.* **149** 451
[13] Bandrauk A, Gauthier J M and McCann J F 1992 *Chem. Phys. Lett.* **200** 399
[14] Charron E, Giusti-Suzor A and Mies F H 1993 *Phys. Rev. Lett.* **71** 692; 1994 *Phys. Rev.* A **49** R641
[15] Nakajima T and Lambropoulos P 1993 *Phys. Rev. Lett.* **70** 1081; 1994 *Phys. Rev.* A **50** 595
[16] Kamiński J Z and Ehlotzky F 1994 *Phys. Rev.* A **50** 4404
[17] Varró S and Ehlotzky F 1988 *Z. Phys.* D **8** 211
[18] Varró S and Ehlotzky F 1993 *Phys. Rev.* A **47** 715
[19] Varró S and Ehlotzky F 1993 *Opt. Commun.* **99** 177
[20] Gordon V 1926 *Z. Phys.* **40** 117
[21] Volkov D V 1935 *Z. Phys.* **94** 250
[22] Varró S and Ehlotzky F 1990 *J. Opt. Soc. Am.* B **7** 537
[23] Berson I Ya and Bondars Kh Ya 1975 *Sov. J. Quantum Electron.* **4** 892
[24] Jahnke, Emde and Lösch 1960 *Tafeln Höherer Funktionen* 6th edn ed F Lösch (Stuttgart: Teubner) p 134